Published in final edited form as:
J Am Chem Soc. 2013 December 26; 135(51): 19075–19078. doi:10.1021/ja4104974.

Heterometallic Triiron-Oxo/Hydroxo Clusters: Effect of Redox-Inactive Metals

David E. Herbert, **Davide Lionetti**, **Jonathan Rittle**, and **Theodor Agapie***
Division of Chemistry and Chemical Engineering, California Institute of Technology, 1200 E California Blvd, Pasadena, California 91125

Abstract

A series of tetranuclear oxo/hydroxo clusters comprised of three Fe centers and a redox-inactive metal (M) of various charge is reported. Crystallographic studies show an unprecedented $Fe_3M(\mu_4\text{-}O)(\mu_2\text{-}OH)$ core that remains intact upon changing M or the oxidation state of iron. Electrochemical studies reveal that the reduction potentials ($E_{1/2}$) span a window of 500 mV and depend upon the Lewis acidity of M. Using the pK_a of the redox-inactive metal aqua complex as a measure of Lewis acidity, these compounds display a linear dependence between $E_{1/2}$ and acidity with a slope of *ca*. 70 mV per pK_a unit. The current study of $[Fe_3MO(OH)]$ and previous ones of $[Mn_3MO_n]$ (n = 2, 4) moieties support the generality of the above relationship between the reduction potentials of heterometallic oxido clusters and the Lewis acidity of incorporated cations, as applied to clusters of different redox-active metals.

The chemistry of synthetic and biological redox centers is affected by Lewis acidic metal ions.[1] A fascinating case in biology is the role of Ca^{2+}, a redox inactive metal in the catalytic site of photosynthetic water oxidation, the heterometallic $CaMn_4O_x$ oxygen-evolving complex (OEC) of photosystem II (PSII).[2] Synthetic Fe^{IV}–oxo complexes show enhanced electron transfer rates and more positive reduction potentials upon addition of redox-inactive Lewis acids such as Sc^{3+} or Ca^{2+}.[3] Group 2 metal ions enhance the rates of dioxygen activation by monometallic Mn^{II} and Fe^{II} complexes.[4] Trivalent redox-inactive Lewis acids (Sc^{3+}, Y^{3+}) facilitate O–O bond cleavage in non-heme iron(III)-peroxo species,[5] and Sc^{3+} modulates O- and H-atom transfer reactivity of a Mn^{IV}-oxo complex.[6] Valence tautomerism is induced by the addition of Zn^{2+} was to $Mn^{V}O$-porphyrinoid complexes.[7] The ligation of redox-inactive metals to pendant donors also affects the reduction potential of oxo-bridged dimanganese species.[8] Alkali and alkali earth metals have also been proposed as components of catalytic clusters in heterogeneous water oxidation by cobalt and manganese oxides.[9]

Synthetic access to well-defined isostructural multimetallic complexes containing different redox-*inactive* metal ions allows systematic investigation of their effects upon the redox-*active* metallic constituents. Our group recently reported a series of heterometallic trimanganese dioxido clusters $[Mn_3M(\mu_4\text{-}O)(\mu_2\text{-}O)]$ (M = Na^+, Ca^{2+}, Sr^{2+}, Zn^{2+}, and Y^{3+}) and demonstrated that the reduction potentials of the clusters are linearly correlated with the Lewis acidity of the redox-inactive metal.[10]

A similar trend was observed for a series of $[Mn^{IV}_3MO_4]$ cubane complexes (M = Ca^{2+}, Sr^{2+}, Zn^{2+}, Sc^{3+}, Mn^{3+}), supported by a multinucleating ligand framework (H_3L, Scheme

*Corresponding Author: agapie@caltech.edu.

Supporting Information. Experimental procedures, spectroscopic characterization, and crystallographic (CIF) data. This material is available free of charge via the Internet at http://pubs.acs.org.

1), that are structurally related to the $CaMn_3O_4$ cubane subsite of the OEC.[11] These studies suggest a role for the Ca^{2+} center in tuning the reduction potential of the active site in PSII. Moreover, the similar trends observed for different cluster structures indicate that this is a general phenomenon in manganese chemistry. It is of interest to determine if the effects discovered in manganese chemistry extend to other transition metals because of the variety of metal oxides studied as catalysts for water oxidation and O_2 reduction.[12] Herein, we describe the synthesis and redox chemistry of a series of heterometallic tetranuclear clusters of iron.

Following synthetic protocols developed with manganese, oxidized heterometallic clusters were targeted from an all-ferrous precursor, $LFe_3(OAc)_3$,[13] supported by a triarylbenzene architecture appended with pyridine and alkoxide donors.[13–14] Treatment of a 1,2-dimethoxyethane (DME) suspension of $LFe^{II}_3(OAc)_3$ and $M(OTf)_2$ (M = Ca, Sr; OTf = trifluoromethanesulfonate) with iodosobenzene (PhIO), followed by crystallization from a CH_2Cl_2/DME solution layered with Et_2O, afforded the all-ferric M-capped complexes **1**-M (M = Ca, Sr) as orange-brown solids (Scheme 1). Single crystal X-ray diffraction (XRD) studies of **1**-M (M = Ca, Sr) revealed that in these complexes, as in $LFe^{II}_3(OAc)_3$, the three iron centers are bridged by three alkoxide donors from L, forming a six-membered ring, and the pyridine nitrogens of each dipyridyloxymethyl moiety coordinate to adjacent metal centers. The apical metal (M) is bridged to the triiron cluster by a μ_4-oxido, to one unique iron center by a μ_2-hydroxo, and to the remaining Fe^{III} centers by bridging acetate moieties. In addition, M is further coordinated by a bidentate DME ligand and a $[OTf]^-$ anion (Fig. 1a–b). Two $[OTf]^-$ ions remain outer-sphere.

The isolated compounds reported here display diagnostic proton nuclear magnetic resonance (^{1}H NMR) spectra, although the paramagnetically broadened and shifted signals have not been assigned (see SI). The zero-field ^{57}Fe Mössbauer spectra of **1**-M (M = Ca, Sr) show features at 80 K that are best modeled as two quadrupole doublets in a 2:1 ratio, consistent with two distinct ferric sites (Fig. 2, S9; Table S1). The long Fe–μ_2-O(5) bond distances [**1**-Ca, 1.881(2); **1**-Sr, 1.884(2) Å] and spectral properties supported the assignment of O(5) as a hydroxo moiety coordinated to an Fe^{III} center of a $Fe^{III}_3MO(OH)$ moiety. In comparison, the Fe–O bond distances for a series of μ_2-hydroxo bridges between Fe^{III} and redox-inactive dications (Ca^{2+}, Sr^{2+}, Ba^{2+}) are between 1.859(2) and 1.872(2) Å.[4b] By contrast, the Fe–O distance in a linear μ_2-oxo bridge between Fe and Sc centers is significantly shorter at 1.754(3) Å.[3a]

The synthetic protocol above likely involves the transfer of two O-atoms from PhIO. This generates a highly reactive Fe^{IV} intermediate capable of H-atom abstraction to form **1**-M. Under similar reaction conditions, related Mn precursors give $Mn^{III}_2Mn^{IV}MO_2$ clusters, likely due to the less oxidizing character of the Mn cluster. The scandium analog of **1**-Ca and **1**-Sr was isolated in the reduced $Fe^{II}Fe^{III}_2$ oxidation state (**2**-Sc). A single crystal XRD study of **2**-Sc revealed an $Fe_3MO(OH)$ core analogous to **1**-Ca and **1**-Sr (Fig. 1c). The assignment of the iron oxidation states was based on the absence of a fourth triflate counteranion, as well as on the observation of a disparity in the Fe–μ_4-O distances in **2**-Sc – two of which (2.005(3), 1.931(3) Å) were similar to those in **1**-Ca and a longer one (2.211(4) Å), consistent with one of the two Fe centers *not* bound to the μ_2-O(H) being more reduced. The presence of a ferrous ion was further confirmed by the zero-field ^{57}Fe Mössbauer spectrum, which showed three distinct features best modeled as one ferrous (δ: 1.135 mm/s) and two ferric (δ: 0.466 mm/s, 0.477 mm/s) quadrupole doublets in a 1:1:1 ratio (Fig. S8), in good agreement with literature values for $Fe^{II/III}$ compounds bearing N/O ligands.[15] The Fe(2)–O(5)H bond in **2**-Sc is elongated compared to **1**-Ca and **1**-Sr likely due to a combination of a more reduced Fe_3 core and a stronger interaction of the bridging moieties with the more Lewis acidic Sc^{3+}. The one-electron reduced Ca compound (**2**-Ca)

was obtained by the chemical reduction of **1**-Ca using one equivalent of cobaltocene ($CoCp_2$; $E^O \sim -1.33$ V vs. Fc/Fc^+) in CH_2Cl_2 (Scheme 1). Crystallization from CH_2Cl_2/Et_2O afforded the reduced compound as confirmed by an XRD study (Fig. 1e). The observed changes in Fe–O distances in **2**-Ca are similar to those of **2**-Sc, with an elongated Fe(2)–O(5)H bond and one long (> 2.1 Å) Fe–μ_4-O distance. The zero-field Mössbauer spectrum collected at 80 K revealed features similar to those of **2**-Sc – two quadrupole doublets in a 1:2 ratio, consistent with one ferrous (δ: 1.166 ^{mm}/s) and two ferric sites (δ: 0.475 ^{mm}/s; Fig. 2).

Complexes containing other redox-inactive metal ions could not be isolated by analogous procedures, possibly due to solubility differences. However, when **1**-Ca was treated with $Zn(OTf)_2$ in CH_3CN (Scheme 1), electrospray ionization mass spectrometry (ESI-MS) of the reaction mixture showed a new species at 1476 *m/z* corresponding to $[LZnFe_3O(OH)(OAc)(OTf)_2]^+$ and the disappearance of signals corresponding to **1**-Ca. A single crystal XRD study of **1**-Zn shows that **1**-Zn retains the $[MFe_3O(OH)]$ moiety, structurally related to **1**-Ca and **1**-Sr, although the smaller zinc center is five-coordinate and binds an aceto-nitrile solvent ligand in place of DME and $[OTf]^-$ (Fig. 1d). Similar to **2**-Sc, **1**-Zn shows a slightly longer Fe(2)–O(5) distance [1.923(4) Å] relative to **1**-Ca and **1**-Sr suggesting that the stronger interaction between μ_2-OH and the more Lewis acidic Zn^{2+} results in a weaker interaction between μ_2-OH and Fe. Under the same reaction conditions using $La(OTf)_3$ instead of $Zn(OTf)_2$ resulted in a product with ^{1}H NMR and Mössbauer spectroscopic features similar to **1**-Ca, **1**-Sr and **1**-Zn (Table S1). This La species was reduced with one equivalent of $CoCp_2$ in CH_2Cl_2 to obtain the one-electron reduced $Fe^{II}Fe^{III}_2$ cluster, **2**-La, which was crystallographically characterized (Fig. 1f). Across the series of $Fe_3MO(OH)$ complexes structurally characterized, Fe(2)-M (and other Fe-M) distances [**1**-Zn, 2.0207(15) Å; **2**-Sc, 3.1638(11) Å; **2**-Ca, 3.3104(18) Å; **1**-Ca, 3.3541(6) Å; **2**-La 3.4159(9) Å; **1**-Sr, 3.5456(4) Å] correlate with the trend of effective ionic radii ($Zn^{2+} < Sc^{3+} < Ca^{2+} < La^{3+} < Sr^{2+}$).[16]

With these complexes in hand, the effect of changing the redox-inactive metals in the clusters was studied electrochemically. Cyclic voltammograms (CV) in CH_2Cl_2/DME (9:1) with 0.1 M NBu_4PF_6 showed quasireversible redox processes assigned as the $[MFe^{III}_3O(OH)]/[MFe^{III}_2Fe^{II}O(OH)]$ couple at potentials of −490 (**1**-Ca), −490 (**1**-Sr), −210 (**1**-Zn), −80 (**1**-La), and +70 mV (**2**-Sc) vs. the ferrocene/ferrocenium couple (Fc/Fc^+) (Fig. 3). Although both **2**-La and **2**-Sc share the same core structure, contain tricationic redox-inactive metals, and have the same overall charge, their reduction potentials differ by ca. 150 mV. The reduction potentials of **1**-Ca and **1**-Sr are similar ($E_{1/2}$ = −490 mV vs. Fc/Fc^+), while the reduction potential of **1**-Zn is more positive by greater than 300 mV ($E_{1/2}$ = −210 mV), even though Zn^{2+} is also a dication. Although there are structural differences at the redox-inactive metal between **1**-Ca/Sr and **1**-Zn (Fig. 1a, b, d), studies of $CaMn_3O_2$ clusters indicated that changes in the coordination sphere at Ca^{2+} do not have a significant effect on the redox chemistry of the cluster.[10] The variation in redox potential observed here for the iron clusters is therefore inconsistent with a purely electrostatic effect. The similarity of the redox potentials of the Ca and Sr variants in comparison to those of the other analogs correlates with the observation that both Sr^{2+} and Ca^{2+} generate catalytically active OEC in PSII (although the activity of the Sr^{2+}-reconstituted active site is lower than that of the native protein).[17]

The $E_{1/2}$ values of the $[Fe^{III}_3MO(OH)]/[MFe^{III}_2Fe^{II}O(OH)]$ and those of previously prepared $[Mn_3MO_2]$ and $[Mn_3MO_4]$ complexes[10–11] were plotted against the pK_a of the metal aqua ions measured in water,[18] used here as a measure of the Lewis acidity of cation M. In all cases, a linear correlation is observed (Fig. 4). Hence, the reduction potentials of the clusters can be tuned by the Lewis acidity of the incorporated redox inactive metal. The

positive shift in reduction potential with increasing Lewis acidity is likely due to the increased electron-withdrawing effect on the bridging oxido/hydroxo ligands, which stabilizes the more reduced iron oxidation state. The distinct effects of the redox-inactive metals is apparent in the different Fe-O(H) distances for both reduced and oxidized clusters (Table S4).

The change in slope between the Fe and Mn [$M'_3MO_2(H)$] clusters (70 vs. 90 mV per pK_a unit, respectively) may reflect the differences in number of oxido ligands, protonation state, metal identity, and oxidation state of the redox-active component. Further studies are necessary for distinguishing these possibilities. The intercepts of the two series are different by *ca*. 400 mV, with the [$Fe^{III}_3MO(OH)$] complexes having more negative reduction potentials than the corresponding [$Mn^{IV-}Mn^{III}_2MO_2$] complexes, consistent with the lower oxidation states for the iron species. The similar linear dependences upon Lewis acidity of the dioxido trimanganese and the oxo/hydroxo triiron complexes suggest that a general correlation exists between the redox potentials of mixed metal oxides and the Lewis acidity of incorporated redox-inactive metals. Such a relationship may provide a quantitative method for tuning the potentials of both homogeneous and heterogeneous metal oxide electrocatalysts by changing the redox-inactive metal in isostructural compounds. The wide range of reduction potentials found within the [$Fe_3MO(OH)$] clusters demonstrates that a large change in the thermodynamics of a catalyst can be effected by redox-inactive metal substitution.

In summary, [$Fe_3MO(OH)$] clusters substituted with divalent and trivalent redox-inactive metals were prepared. A systematic study of the electrochemical effect of the Lewis acidic metal ions on the iron cluster reduction potentials was carried out. Varying the Lewis acidity of the capping metal from Ca^{2+} to Sc^{3+} shifted the redox potentials of these clusters by over 500 mV. These results support the generality of the role redox-inactive metals can play in modulating the redox potential of the redox-active centers via μ_4-oxo and/or μ_2-hydroxo ligands. Current studies are focused on the effects of redox-inactive metals on the physical properties and chemical reactivity of other metal-oxido compounds of varying structure, metal character, oxidation state and oxido content to better understand the fundamental basis for multi-electron, multi-proton catalysis by complex metal clusters.

Supplementary Material

Refer to Web version on PubMed Central for supplementary material.

Acknowledgments

This work was supported by the California Institute of Technology, the Searle Scholars Program, the NSF CAREER CHE-1151918 (T.A.), a Camille & Henry Dreyfus Environmental Chemistry Fellowship (D.E.H.), and a Resnick Sustainability Institute graduate fellowship (D.L.). T.A. is a Sloan and Cottrell Fellow. We thank Larry M. Henling and Dr. Michael Takase for assistance with crystallography and Prof. Jonas C. Peters for use of a Mössbauer spectrometer. The Bruker KAPPA APEXII X-ray diffractometer was purchased via an NSF Chemistry Research Instrumentation award to Caltech (CHE -0639094). We acknowledge the Gordon and Betty Moore Foundation, the Beckman Institute, and the Sanofi-Aventis BRP at Caltech for their generous support of the Molecular Observatory at Caltech. Operations at SSRL are supported by the US DOE and NIH.

References

1. (a) Fukuzumi S, Ohkubo K. Coord Chem Rev. 2010; 254:372.(b) Fukuzumi, S. In Prog Inorg Chem. Karlin, KD., editor. Vol. 56. John Wiley & Sons Inc; New York: 2009. p. 49
2. (a) Yocum CF. Coord Chem Rev. 2008; 252:296.(b) Umena Y, Kawakami K, Shen JR, Kamiya N. Nature. 2011; 473:55. [PubMed: 21499260] (c) Ferreira KN, Iverson TM, Maghlaoui K, Barber J, Iwata S. Science. 2004; 303:1831. [PubMed: 14764885]

3. (a) Fukuzumi S, Morimoto Y, Kotani H, Naumov P, Lee YM, Nam W. Nat Chem. 2010; 2:756. [PubMed: 20729896] (b) Morimoto Y, Kotani H, Park J, Lee YM, Nam W, Fukuzumi S. J Am Chem Soc. 2011; 133:403. [PubMed: 21158434]
4. (a) Park YJ, Ziller JW, Borovik AS. J Am Chem Soc. 2011; 133:9258. [PubMed: 21595481] (b) Park YJ, Cook SA, Sickerman NS, Sano Y, Ziller JW, Borovik AS. Chem Sci. 2013; 4:717. [PubMed: 24058726]
5. (a) Li F, Van Heuvelen KM, Meier KK, Muenck E, Que L Jr. J Am Chem Soc. 2013; 135:10198. [PubMed: 23802702] (b) Lee YM, Bang S, Kim YM, Cho J, Hong S, Nomura T, Ogura T, Troeppner O, Ivanovic-Burmazovic I, Sarangi R, Fukuzumi S, Nam W. Chem Sci. 2013; 4:3917.
6. Chen J, Lee YM, Davis KM, Wu X, Seo MS, Cho KB, Yoon H, Park YJ, Fukuzumi S, Pushkar YN, Nam W. J Am Chem Soc. 2013; 135:6388. [PubMed: 23324100]
7. Leeladee P, Baglia RA, Prokop KA, Latifi R, de Visser SP, Goldberg DP. J Am Chem Soc. 2012; 134:10397. [PubMed: 22667991]
8. (a) Horwitz CP, Ciringh Y, Weintraub ST. Inorg Chim Acta. 1999; 294:133.(b) Horwitz CP, Ciringh Y. Inorg Chim Acta. 1994; 225:191.
9. (a) Risch M, Klingan K, Ringleb F, Chernev P, Zaharieva I, Fischer A, Dau H. Chem Sus Chem. 2012; 5:542.(b) Zaharieva I, Najafpour MM, Wiechen M, Haumann M, Kurz P, Dau H. Energy Environ Sci. 2011; 4:2400.(c) Wiechen M, Zaharieva I, Dau H, Kurz P. Chem Sci. 2012; 3:2330.(d) Najafpour MM, Pashaei B, Nayeri S. Dalton Trans. 2012; 41:4799. [PubMed: 22382465] (e) Najafpour MM, Ehrenberg T, Wiechen M, Kurz P. Angew Chem Int Ed. 2010; 49:2233.
10. Tsui EY, Tran R, Yano J, Agapie T. Nat Chem. 2013; 5:293. [PubMed: 23511417]
11. (a) Tsui EY, Agapie T. Proc Natl Acad Sci USA. 2013; 110:10084. [PubMed: 23744039] (b) Kanady JS, Tsui EY, Day MW, Agapie T. Science. 2011; 333:733. [PubMed: 21817047]
12. (a) Singh A, Spiccia L. Coord Chem Rev. 2013; 257:2607.(b) Bockris JO, Otagawa T. J Electrochem Soc. 1984; 131:290.(c) Cheng FY, Chen J. Chem Soc Rev. 2012; 41:2172. [PubMed: 22254234] (d) Neburchilov V, Wang HJ, Martin JJ, Qu W. J Power Sources. 2010; 195:1271.
13. Tsui EY, Kanady JS, Day MW, Agapie T. Chem Commun. 2011; 47:4189.
14. Tsui EY, Day MW, Agapie T. Angew Chem Int Ed. 2011; 50:1668.
15. (a) Reynolds RA, Coucouvanis D. Inorg Chem. 1998; 37:170.(b) Schmitt W, Anson CE, Pilawa B, Powell AK. Z Anorg Allg Chem. 2002; 628:2443.(c) Chardon-Noblat S, Horner O, Chabut B, Avenier F, Debaecker N, Jones P, Pecaut J, Dubois L, Jeandey C, Oddou JL, Deronzier A, Latour JM. Inorg Chem. 2004; 43:1638. [PubMed: 14989656] (d) Singh AK, Jacob W, Boudalis AK, Tuchagues JP, Mukherjee R. Eur J Inorg Chem. 2008:2820.(e) Lalia-Kantouri M, Papadopoulos CD, Hatzidimitriou AC, Bakas T, Pachini S. Z Anorg Allg Chem. 2010; 636:531.
16. Shannon RD. Acta Crystallogr A. 1976; 32:751.
17. Ghanotakis DF, Babcock GT, Yocum CF. FEBS Lett. 1984; 167:127.
18. Perrin, DD. Ionisation Constants of Inorganic Acids and Bases in Aqueous Solution. Pergamon Press; New York: 1982.

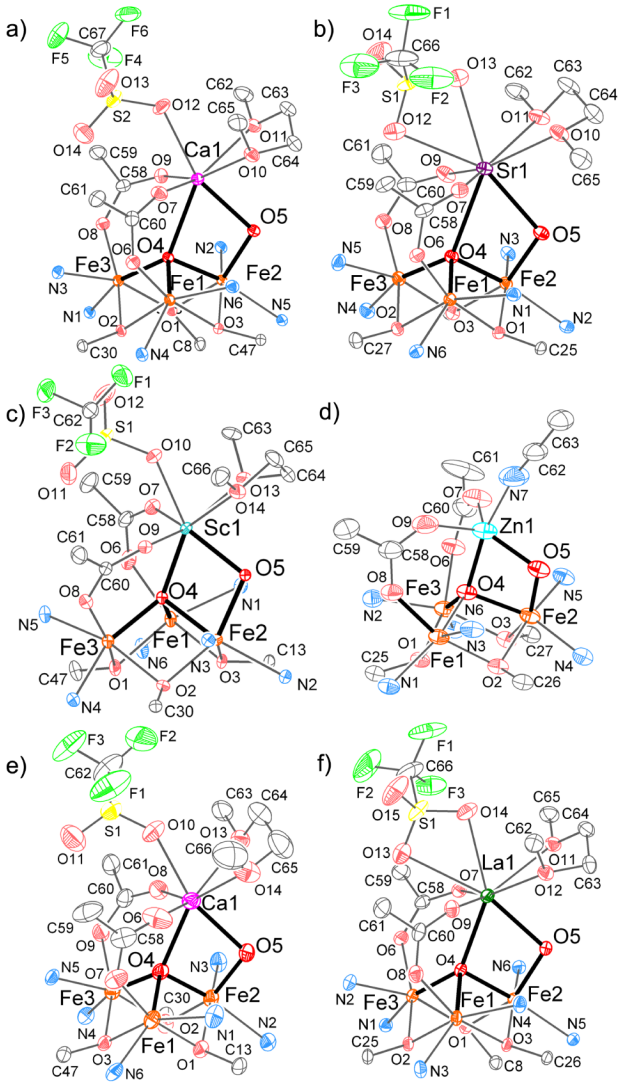

Figure 1.

Truncated solid-state structures of (a) **1**-Ca, (b) **1**-Sr, (c) **2**-Sc, (d) **1**-Zn, (e) **2**-Ca and (f) **2**-La. Portions of the ligand (L), hydrogen atoms and outer-sphere anions are omitted for clarity. Thicker lines emphasize the $[MFe_3O_2]$ moiety.

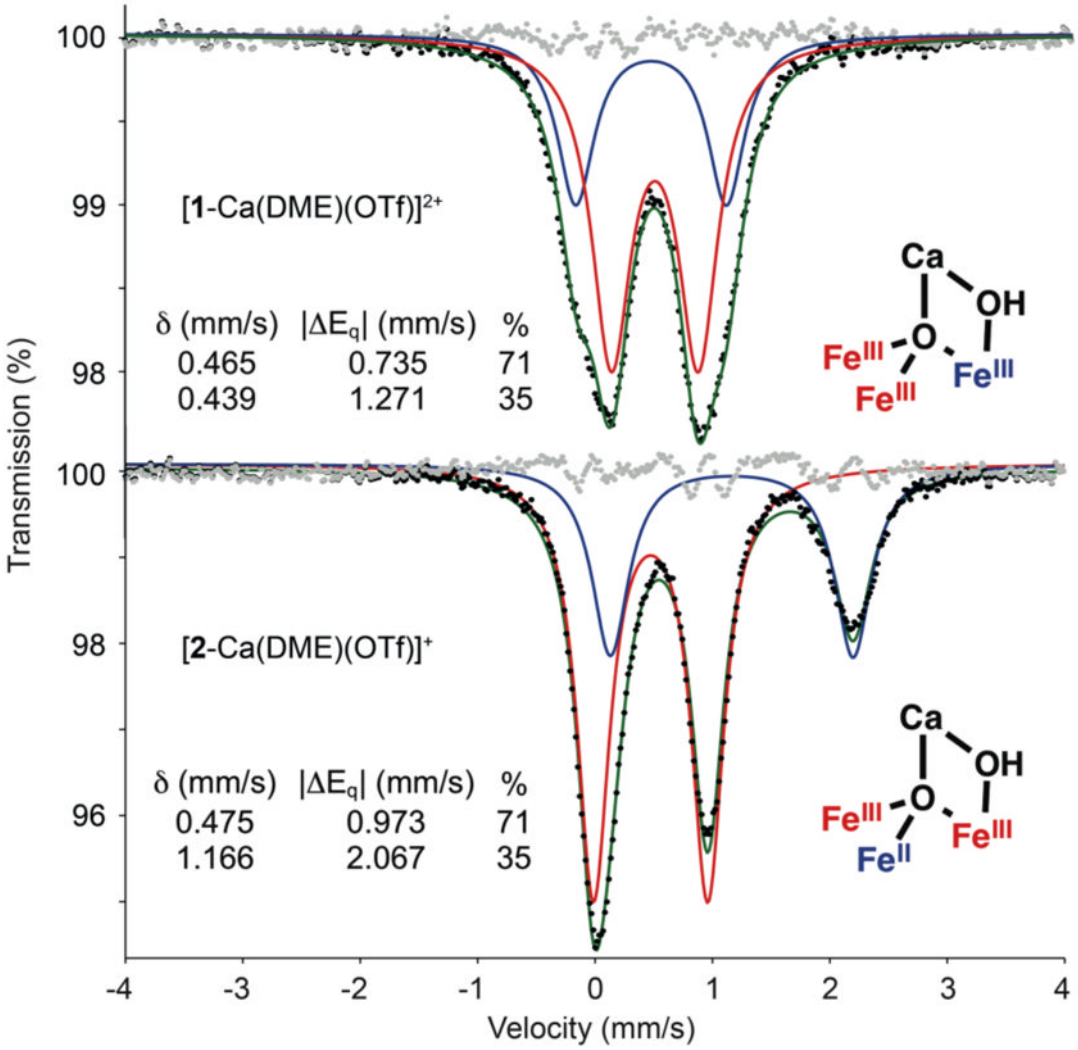

Figure 2.
Zero-field ^{57}Fe Mössbauer spectra for **1**-Ca and **2**-Ca: (80 K, data: black dots, spectral fit: green line, deconvolution: red and blue lines; residual: grey dots.

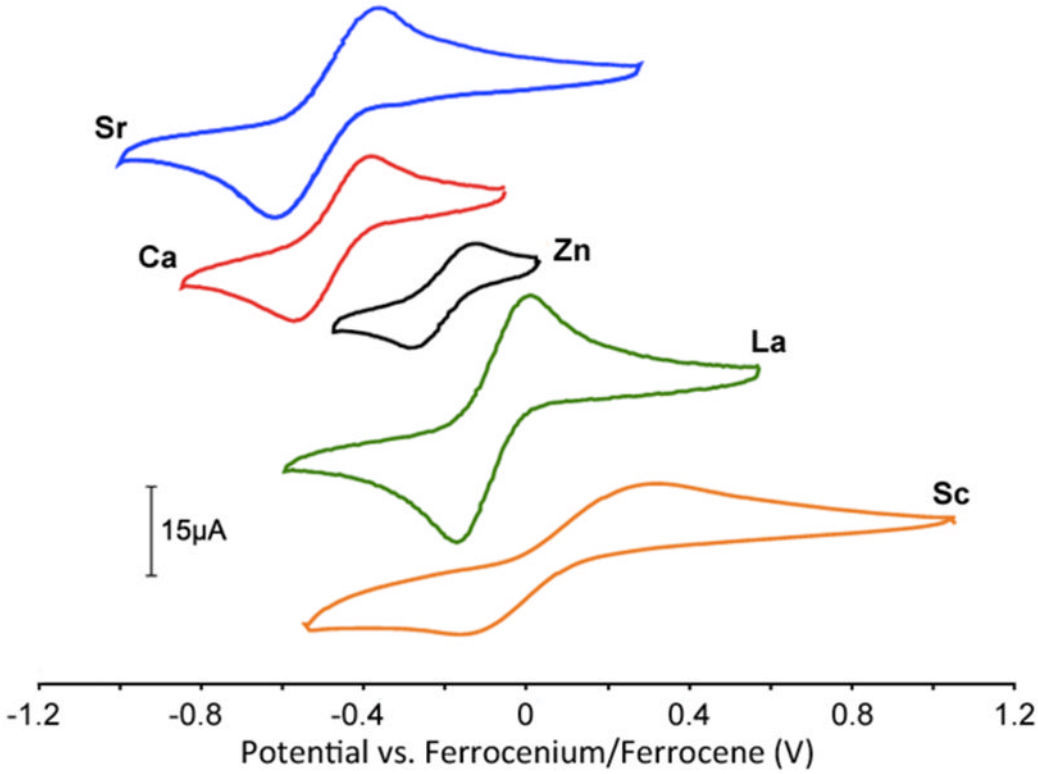

Figure 3.

Cyclic voltammograms corresponding to the $[MFe^{III}_3O(OH)]/[MFe^{III}_2Fe^{II}O(OH)]$ redox couple (M = Sc^{3+}, La^{3+}, Zn^{2+}, Ca^{2+}, and Sr^{2+}) in 0.1 M NBu_4PF_6 in CH_2Cl_2/1,2-DME (9:1). Scan rate of 200 mV/s. Potentials are referenced to Fc/Fc^+.

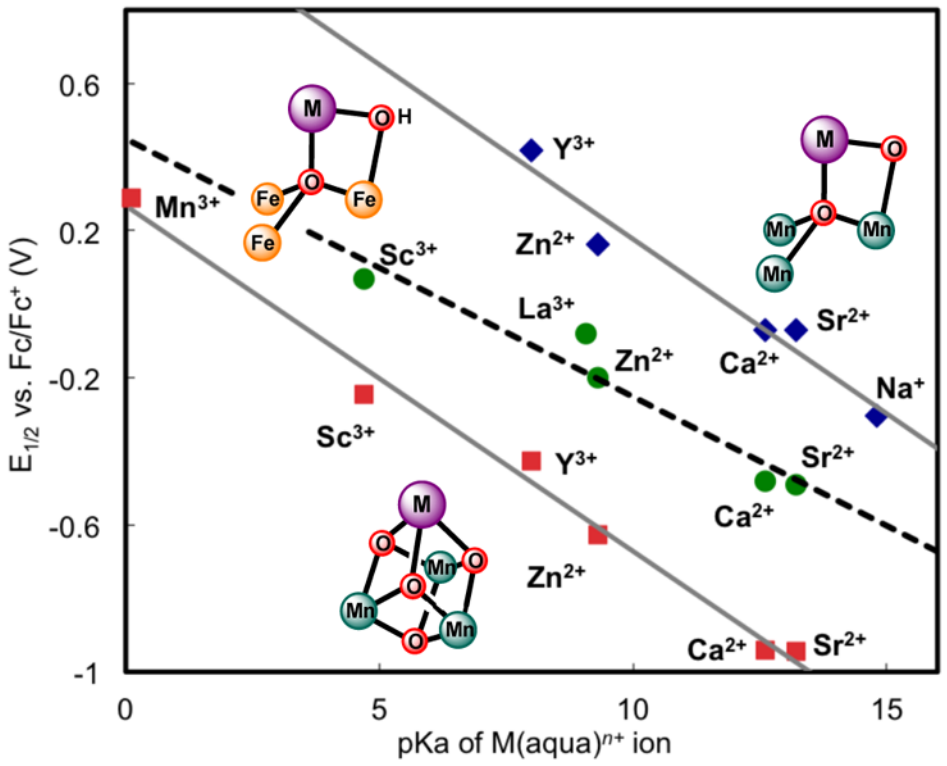

Figure 4.

Reduction potentials of $MFe_3O(OH)$ complexes (green circles), MMn_3O_2 complexes[10] (blue diamonds), and MMn_3O_4 complexes[11a] (red squares) vs. pK_a of the corresponding M(aqua)$^{n+}$ ion as a measure of Lewis acidity. Potentials were referenced to Fc/Fc^+.

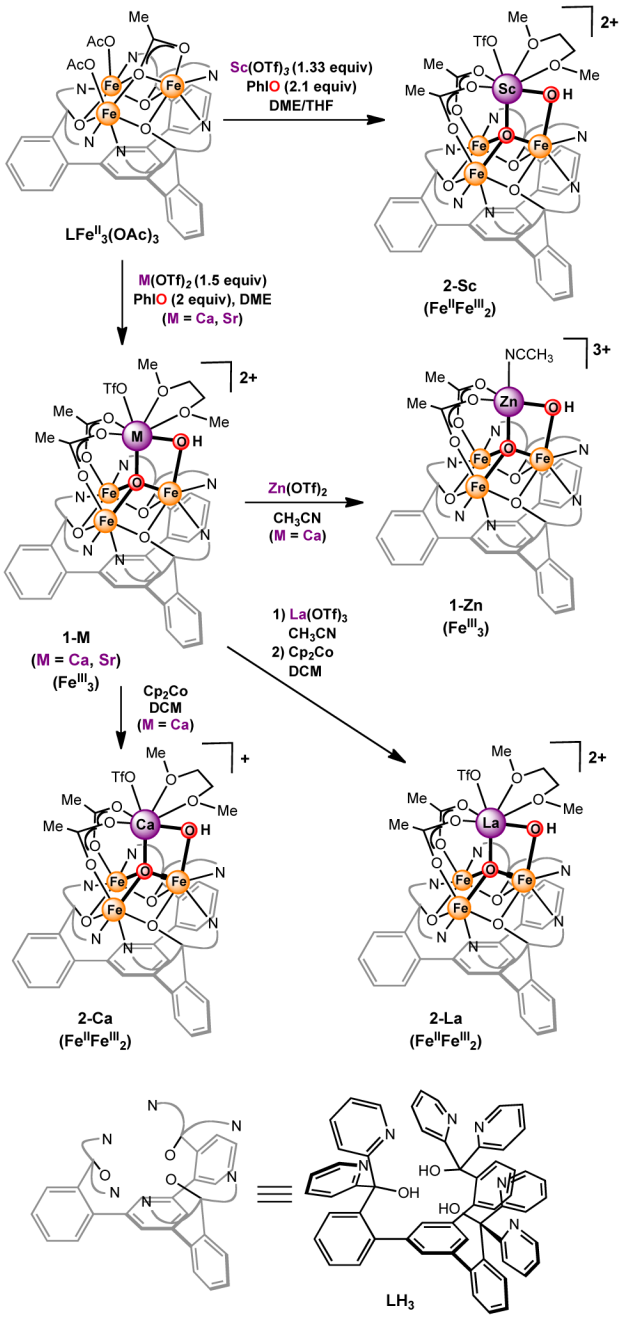

Scheme 1.

Synthesis of complexes **1**-M (M = Ca, Sr, Zn), **2**-M (M = Ca, Sc, La).